A Fluorescence Method To Define Transmembrane α-Helices in Membrane Proteins: Studies with Bacterial Diacylglycerol Kinase†

Jiraphun Jittikoon, J. Malcolm East, and Anthony G. Lee*

School of Biological Sciences, University of Southampton, Southampton SO16 7PX, U.K.

Received May 1, 2007; Revised Manuscript Received July 12, 2007

ABSTRACT: Hydropathy plots have problems in identifying the sequences of transmembrane (TM) α-helices when they contain charged residues. Here we show that fluorescence spectroscopy can be used to define the ends of TM α-helices. Diacylglycerol kinase (DGK) from *Escherichia coli* contains three transmembrane (TM) α-helices per monomer. We have used fluorescence techniques to define the region of the putative first TM helix (TM1) that spans the hydrophobic core of the lipid bilayer surrounding DGK in reconstituted membranes. Single Cys mutants were introduced into TM1 and flanking sites, in a mutant of DGK lacking the two native Cys residues. Introduction of Cys residues into the region between residues 28 and 34 resulted in mutants with low activities, due to a combination of reduced affinities for ATP and diacylglycerol and a reduced maximum rate. Cross-linking experiments showed that the low-activity mutants were present largely in the normal, trimeric form after reconstitution. Fluorescence emission maxima for the Cys mutants labeled with *N*-((2-(iodoacetoxy)ethyl)-*N*-methyl)amino-7-nitrobenz-2-oxa-1,3-diazole (IANBD) reconstituted into bilayers of dioleoylphosphatidylcholine varied with position, suggesting that the region of TM1 spanning the hydrophobic core of the bilayer runs from Glu-28 on the cytoplasmic side to Asp-49 or Val-50 on the periplasmic side. This locates the charged/polar cluster ^{32}RQE^{34} within the hydrophobic core of the bilayer. Fluorescence quenching experiments agree with this assignment for TM1, the results showing a periodicity consistent with distinct stripes of amino acid residues along the length of the helix, the stripes facing the lipid bilayer and facing the rest of the protein, respectively. The residues located close to the glycerol backbone region of the bilayer remained the same when the lipid fatty acyl chain length was changed in the range C14 to C22, showing that hydrophobic matching between the protein and the surrounding lipid bilayer is highly efficient.

An important feature of intrinsic membrane protein structure is how the protein sits in the lipid bilayer; interactions between a membrane protein and the surrounding lipid bilayer help to shape the protein and so affect its function (*1*, *2*). Unfortunately, most high-resolution structures of membrane proteins contain few, if any, lipid molecules, most lipid molecules being lost either during purification or during crystallization from detergent, or being too disordered to be resolved in the crystal structure. Since transmembrane (TM[1]) α-helices usually extend beyond the hydrophobic core of the lipid bilayer into the polar lipid headgroup region and beyond, it is difficult to identify the likely position of the lipid bilayer around the protein in the absence of a large number of lipid molecules, although recent theoretical approaches have improved the situation (*3*). The problem of identifying the position of the lipid bilayer around a membrane protein is, of course, more severe when a high-resolution structure is not available; hydropathy plots will usually identify the TM α-helices in a membrane protein but cannot exactly define the regions of the helices that span the hydrophobic core of the lipid bilayer. The problem is particularly acute for TM α-helices containing charged residues close to the ends of the helices that can "snorkel" up to the surface of the bilayer, locating the charge group of the amino acid residue in the polar lipid headgroup region. For example, the first TM α-helix of the Ca^{2+}-ATPase of sarcoplasmic reticulum contains four acidic residues toward the N-terminus of the hydrophobic core spanning region of the helix, so that the start of the helix is incorrectly identified in hydropathy plots (*4*). Similarly, the third TM α-helix of the Ca^{2+}-ATPase contains a Lys residue seven residues from the N-terminus of the region of the helix that spans the hydrophobic core of the bilayer, again making correct identification of the ends of the helix difficult (*4*).

Given these problems, it is important to have experimental methods that can be used in combination with hydropathy plots to identify the probable location of the lipid bilayer around a membrane protein. In previous studies we have shown that the environmental sensitivity of fluorescence emission of the Trp residue can be used to identify the ends of transmembrane α-helices (*5*). However, this approach is limited by the requirement to produce a functional Trp-free

† We thank The Royal Thai Government for a studentship (to J.J.).

* To whom correspondence should be addressed. Phone: 44 (0) 2380 594331. Fax: 44 (0) 2380 594459. E-mail: agl@soton.ac.uk.

[1] Abbreviations: TM, transmembrane; DGK, diacylglycerol kinase; di(C14:1)PC, dimyristoleoylphosphatidylcholine; di(C16:1)PC, dipalmitoleoylphosphatidylcholine; di(C18:1)PC, dioleoylphosphatidylcholine; di(C20:1)PC, dieicosenoylphosphatidylcholine; di(C22:1)PC, dierucoylphosphatidylcholine; DHG, 1,2-dihexanoylglycerol; SDS−PAGE, sodium dodecyl sulfate−polyacrylamide gel electrophoresis. Tempo, 2,2,6,6-tetramethylpiperidine-1-oxyl; IANBD, *N*-((2-(iodoacetoxy)-ethyl)-*N*-methyl)amino-7-nitrobenz-2-oxa-1,3-diazole; DM, *n*-decyl β-D-maltopyranoside.

10.1021/bi7008213 CCC: $37.00
Published on Web 08/28/2007

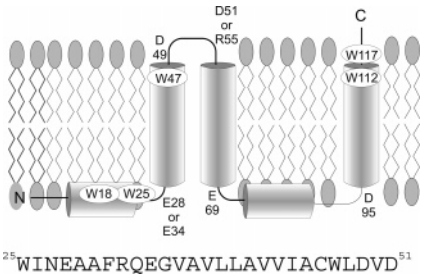

FIGURE 1: Predicted structure of DGK showing probable positions of Trp residues and TM α-helices with the residues likely to span the hydrophobic core of the helices. Also shown is the amino acid sequence around the first TM α-helix.

mutant into which single Trp residues can be introduced at chosen, defined positions. Since membrane proteins generally contain fewer Cys residues than Trp residues, it will generally be easier to obtain functional Cys-free mutants than Trp-free mutants, and Cys residues can be made fluorescent by labeling with a variety of fluorophors that show environmental sensitivity (*6*).

Here we use the Cys labeling approach to define the location of the first TM α-helix of diacylglycerol kinase (DGK) of *Escherichia coli* (Figure 1). DGK is the smallest known kinase and is predicted to contain three TM α-helices with two amphipathic helices on the cytoplasmic side of the membrane (*7*). It forms a homotrimeric structure with three active sites per trimer, the active sites being at subunit−subunit interfaces (*7*, *8*), with the second TM α-helix being most involved in trimer contacts (*9*). DGK catalyzes the reaction

$$\text{diacylglycerol} + \text{ATP} \leftrightarrows \text{phosphatidic acid} + \text{ADP}$$

and shows simple Michaelis−Menten kinetics with respect to both ATP and diacylglycerol, the mechanism involving direct phosphoryl transfer from ATP to diacylglycerol (*10*, *11*). It has been suggested that all five Trp residues in each DGK monomer are located close to the glycerol backbone region of the lipid bilayer (*12*), as shown in Figure 1.

For many membrane proteins of known three-dimensional structure, the ends of the regions of the TM α-helices that span the hydrophobic core of the bilayer are marked by acidic residues (*2*). Of the three predicted TM α-helices of DGK, the core-spanning region of the second helix TM2 is probably defined by Asp-51 or Arg-55 at the N-terminal end and Glu-69 at the C-terminal end (Figure 1) and that of TM3 is probably defined by Asp-95 at the N-terminal end and Trp-112 at the C-terminal end (*12*). However, although the C-terminal end of TM1 is probably defined by Asp-49, the N-terminal end is unclear, and could be either Glu-28 or Glu-34. Favoring Glu-28 as the marker for the N-terminal end are the facts that Glu-28 is conserved whereas Glu-34 is not, that a helix defined by Glu-34 and Asp-49 would be unusually short for a lipid-exposed helix (*13*), and that NMR studies suggest that residues 29−47 are helical (*14*). Here we show that it is possible to identify the ends of TM1 using a fluorescence approach.

MATERIALS AND METHODS

Materials and General Procedures. Dimyristoleoylphosphatidylcholine [di(C14:1)PC], dipalmitoleoylphosphatidylcholine [di(C16:1)PC], dioleoylphosphatidylcholine [di(C18:1)PC], dieicosenoylphosphatidylcholine [di(C20:1)PC], and dierucoylphosphatidylcholine [di(C22:1)PC] were obtained from Avanti Polar Lipids. 2,2,6,6-Tetramethylpiperidine-1-oxyl (Tempo) and 16-doxyl stearic acid were obtained from Aldrich, and *N*-((2-(iodoacetoxy)ethyl)-*N*-methyl)amino-7-nitrobenz-2-oxa-1,3-diazole (IANBD) was obtained from Molecular Probes.

A plasmid expressing wild-type His-tagged DGK was generously provided by Professor James Bowie of UCLA. DGK was purified as described in Pilot et al. (*13*). In brief, cells were pelleted by centrifugation at 12000*g* for 10 min and then resuspended in buffer (50 mM sodium phosphate, 0.3 M NaCl, pH 7.5) containing 1 mM 4-(2-aminoethyl)-benzenesulfonyl fluoride (AEBSF) and 3% (w/v) octylglucoside, followed by stirring at 0 °C for 2 h. The solubilized protein was absorbed onto Ni-NTA-agarose resin (Quiagen). The resin was washed with buffer containing 1.5% octylglucoside and 3 mM imidazole, and then packed into a column. The column was washed with buffer containing 1.5% octylglucoside and 3 mM imidazole and then with buffer containing 0.5% *n*-decyl β-D-maltopyranoside (DM). DGK was eluted from the column with buffer containing 0.5% DM and 0.25 M imidazole. The eluted protein gave a single band on SDS−polyacrylamide gel electrophoresis. Samples were concentrated to 6−10 mg of protein/mL using a Vivaspin 500 concentrator (molecular weight cutoff 10 000) and then flash-frozen in liquid nitrogen at −80 °C. It was found that freezing samples at concentrations below ca. 4 mg/mL led to loss of activity. Protein concentrations were estimated using an extinction coefficient of 30 800 M^{-1} cm^{-1} at 280 nm.

Site directed mutagenesis was performed using the Quikchange protocol from Stratagene. The mutants were confirmed by DNA sequencing.

Purified DGK was reconstituted into lipid bilayers by mixing lipid and DGK in cholate followed by dilution to decrease the concentration of cholate below its critical micelle concentration (*13*). For measurements of activity, phospholipid (8 μmol) and the desired concentration of DHG were dried from a chloroform solution onto the walls of a thin glass vial. Buffer (400 μL; 60 mM Pipes, pH 6.9) containing 28 mM cholate was added, and the sample was sonicated to clarity in a bath sonicator (Ultrawave). DGK (1.5 nmol; 22 μg) was added and the sample left at room temperature for 15 min to equilibrate, followed by incubation on ice until use; the molar ratio of lipid:DGK was 6000:1. Twenty microliters of the sample was then diluted into 1 mL of the assay buffer described below to re-form membranes, representing a 50-fold dilution. A high molar ratio of lipid:DGK was used in these experiments to ensure that a sufficiently high molar ratio of the DHG substrate to DGK was present in the membranes for steady-state kinetics to be measurable over a time period of several minutes (*13*). For fluorescence measurements, the same protocol was used, except that lipid (2 μmol) was reconstituted with DGK (20 nmol) to give a molar ratio of lipid:DGK of 100:1.

Steady-State Kinetics. For activity measurements, DHG at the required concentration was included with the phospholipid at the reconstitution stage, as described above. DGK activity was measured using a coupled enzyme assay (*13*). The assay medium consisted of buffer (60 mM Pipes, pH 6.9) containing phosphoenolpyruvate (2 mM), NADH (0.2

mM), ATP (5 mM), Mg^{2+}(20 mM), pyruvate kinase (18 units), and lactate dehydrogenase (22 units). The mixture was incubated at 25 °C for 10 min to ensure that any residual ADP in the ATP sample was consumed. The assay was initiated by addition of DGK (1.5 μg) to 1 mL of the assay medium, and the oxidation of NADH was monitored by the decrease in absorbance at 340 nm. Quoted rates are the averages of triplicate measurements on two separate reconstitutions.

The rate v for DHG for an enzyme with a two substrate, random equilibrium mechanism is given by

$$v = \frac{v_{max}[A][B]}{\alpha K_A K_B + \alpha K_A[B] + \alpha K_B[A] + [A][B]} \quad (1)$$

where A and B are MgATP and DHG, respectively, K_A and K_B are dissociation constants for MgATP and DHG respectively, and α is the factor by which the dissociation constant of one substrate is modified by the prior binding of the other substrate (*10*, *15*). Although the best fit to eq 1 was obtained for a value of α of 0.45, suggesting a low level of cooperativity, a good fit was also obtained with a value of α of 1 (*10*). Assuming a value for α of 1 allows a considerable simplification of eq 1 (*15*). In experiments in which the concentration of A is varied with that of B being held constant, the rate is given by

$$v = v_{max}^{app}[A]/(K_A + [A]) \quad (2)$$

where

$$v_{max}^{app} = \frac{v_{max}}{\left(1 + \frac{K_B}{[B]}\right)} \quad (3)$$

with a corresponding set of equations for the experiment where the concentration of B is varied with that of A held constant.

Data were fitted to eqs 2 and 3 using the nonlinear least-squares routine in the SigmaPlot package.

Labeling of DGK. Cys-containing mutants of DGK were labeled with IANBD by incubating DGK (ca. 5 mg/mL) in PBS buffer (140 mM NaCl, 2.7 mM KCl, 10 mM Na_2HPO_4, 1.8 mM KH_2PO_4, pH 7.2) containing tri(2-carboxyethyl)-phosphine hydrochloride (3 mM) with a 5-fold molar excess of IANBD, added as a stock solution (10 mg/mL in dimethyl sulfoxide), for 45 min at 25 °C. The reaction mixture contained ca. 0.5% DM. Unreacted label was removed on a G-25 Sepharose column. Labeling ratios were determined from measured absorbances at 280 and 478 nm, corresponding to Trp and the NBD group, respectively, with extinction coefficients of 30 800 M^{-1} cm^{-1} and 25 000 M^{-1} cm^{-1}.

Fluorescence Measurements. Fluorescence of NBD-labeled DGK was recorded for 1.0 μM DGK with excitation at 478 nm, using an SLM 8000C fluorimeter (Urbana IL), at 25 °C. Fluorescence emission spectra were corrected for light scatter by subtraction of a blank consisting of lipid alone in buffer. To obtain accurate values for wavelengths of maximum fluorescence emission, intensity corrected fluorescence spectra were fitted to skewed Gaussian curves (*12*). In quenching experiments with iodide, a stock solution of 1 M KI in buffer containing 100 mM $Na_2S_2O_3$ was added to DGK (0.98 μM) in buffer containing KCl at a concentration chosen to maintain the total concentration KI + KCl at 0.91 M. In quenching experiments with Tempo, a stock solution of 10 mM Tempo in buffer (20 mM Hepes, 100 mM KCl, 1 mM EGTA, pH 7.2) was added to DGK (1 μM) to give a final concentration of Tempo of 2 mM. For quenching experiments with 16-doxyl stearic acid, the 16-doxyl stearic acid was mixed with di(C18:1)PC in chloroform to give 15 mol % 16-doxyl stearic acid; the mixture was then dried down and reconstituted with DGK as described above. Fluorescence intensities were measured at 525 nm.

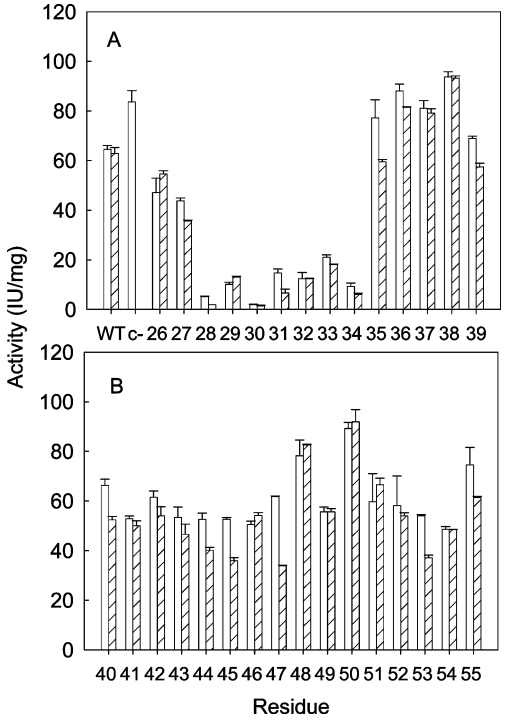

FIGURE 2: Activities for Cys mutants of DGK reconstituted into di(C18:1)PC. Activities (IU/mg protein) are shown for wild type DGK (WT), for the Cys-free mutant (c-) and for mutants with single Cys residues at positions 26−39 (A) and 40−55 (B). Open and closed bars correspond to unlabeled and NBD-labeled DGK respectively. Activities were measured at 20 mol % DHG and 5 mM ATP.

Glutaraldehyde Cross-Linking. DGK was reconstituted into di(C18:1)PC at a molar ratio of lipid:DGK of 100:1. Samples (28 μg of DGK) were incubated with glutaraldehyde (25 mM) in buffer (60 mM Pipes, pH 6.9) containing 0.5 mM dithiothreitol with shaking for 16 h. Reactions were terminated by dilution into SDS−PAGE loading buffer. Cross-linked products were loaded onto 15% gels and analyzed using SDS−PAGE using standard procedures. % trimer formation was estimated by comparing the intensity of the trimer band in SDS−PAGE with that observed on cross-linking wild type DGK, taken as 100%.

RESULTS

Expression of Mutants. Wild type DGK contains two Cys residues, at positions 46 and 113. The Cys-less double mutant C46A,C113A has been reported to be fully active (*9*). We similarly found that the Cys-less double mutant C46A,C113L was active (Figure 2) and used this to construct a series of single Cys mutants, covering the range between residues 26 to 55, including all the residues likely to be in TM1 and in

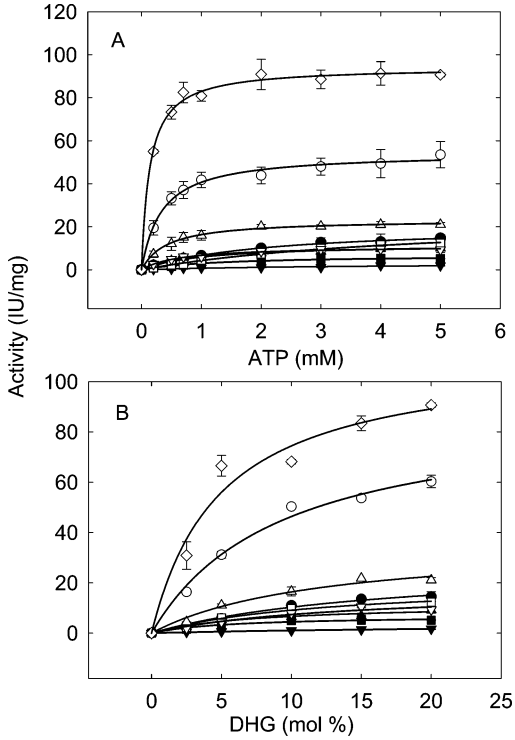

FIGURE 3: Activities for low-activity mutants of DGK in di(C18:1)PC. Activities (IU/mg) were determined in the presence of 20 mol % DHG as a function of ATP concentration (A), or in the presence of 5 mM ATP as a function of DHG concentration (B). The mutants were as follows: (○) WT; (◇) Cys-less mutant; (■) E28C; (▲) A29C; (▼) A30C; (●) F31C; (□) R32C; (△) Q33C; (▽) E34C. The solid lines show fits to eqs 2 and 3, giving the values for K_m and v_{max} listed in Table 1.

the loop linking TM1 to TM2 (Figure 1). All expressed in *E. coli* to comparable levels.

Activities of Mutant DGKs. Mutants were reconstituted into bilayers of di(C18:1)PC, and the rate of ATP hydrolysis was assayed at 20 mol % DHG in the membrane, at an ATP concentration of 5 mM (Figure 2). The activity of the Cys-less mutant C46A,C113L was higher than that of wild type DGK when assayed under these conditions (Figure 2) due to higher values for v_{max} and lower values for K_M for both ATP and DHG (Figure 3; Table 1). Activities for single Cys mutants from residues 35 to 55 were generally similar to those of wild type, whereas single Cys mutations at residues from 28 to 34 resulted in very low activities under these assay conditions. For those mutants where comparison is possible, activities reported in Figure 2 are similar to those obtained by Gorzelle et al. (*16*) and Oxenoid et al. (*14*) following reconstitution.

Activities for mutants at positions 28 to 34 were measured as a function of concentrations of ATP and DHG and compared to the activities for wild type DGK and for the Cys-less mutant (Figure 3). All data fitted well to eqs 2 and 3 for a random equilibrium mechanism, and values for v_{max} estimated from experiments in which ATP was the variable agreed within experimental error with estimates from experiments in which DHG was the variable (Table 1), giving confidence in the method of analysis.

Cross-Linking Experiments. Cross-linking wild type DGK in detergent micelles with glutaraldehyde gives a characteristic pattern in SDS−PAGE with a predominant band representing the cross-linked trimer, with faint bands for

Table 1: Activities of Cys Mutants of DGK in di(C18:1)PC[a]

		substrate			
		ATP		DHG	
mutant	% trimer compared to WT	K_M (mM)	v_{max} (IU/mg)	K_M (mol %)	v_{max} (IU/mg)
WT	100	0.34 ± 0.03	79.4 ± 1.6	9.2 ± 1.8	95.3 ± 8.7
c-		0.13 ± 0.01	117.1 ± 1.5	4.9 ± 1.7	114.0 ± 12.9
E28C	93	1.3 ± 0.2	8.9 ± 0.4	5.7 ± 2.2	8.9 ± 1.0
A29C	64	1.0 ± 0.2	16.3 ± 0.9	7.4 ± 2.9	14.0 ± 2.1
A30C	79	3.3 ± 1.6	7.3 ± 1.6	27.2 ± 7.9	6.5 ± 1.2
F31C	72	2.1 ± 0.2	38.3 ± 1.5	17.2 ± 4.5	39.9 ± 5.6
R32C	63	4.8 ± 0.6	40.9 ± 3.3	12.9 ± 4.6	40.9 ± 7.6
Q33C	77	0.4 ± 0.1	37.3 ± 0.6	12.1 ± 4.2	39.0 ± 6.5
E34C	100	0.6 ± 0.1	18.5 ± 0.6	13.7 ± 7.1	19.8 ± 5.2

[a] Data in Figures 3A and 3B were fitted to eqs 2 and 3 to give the values for v_{max} and for K_m for ATP and DHG listed in the table. In experiments with ATP as the variable, the concentration of DHG was 20 mol %; in experiments with DHG as the variable, the concentration of ATP was 5 mM. As shown, the estimates for v_{max} obtained from the two sets of experiments agree within experimental error. % trimer was determined from glutaraldehyde cross-linking experiments, measured relative to the amount of trimer formed after cross-linking wild type DGK. c- refers to the Cys-less mutant of DGK.

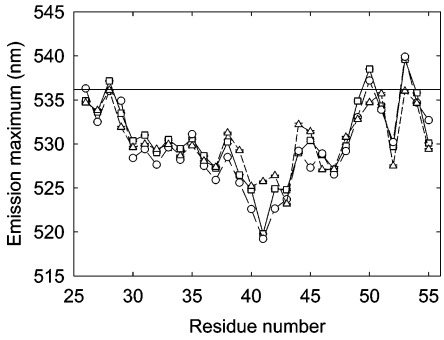

FIGURE 4: Fluorescence properties of NBD-labeled DGK. Fluorescence emission maxima (nm) are plotted as a function of the label position for DGK reconstituted into (□; solid line) di(C14:1)PC; (○; broken line) di(C18:1)PC; (△; dotted line) di(C22:1)-PC. The horizontal line at 536.2 nm marks the expected fluorescence emission maximum for an NBD group located immediately below the glycerol backbone region of the bilayer.

monomer and dimer (*16*). A similar result was obtained for DGK reconstituted in di(C18:1)PC, and Table 1 lists the amount of trimer formation observed after glutaraldehyde cross-linking for the low-activity mutants of DGK compared to that observed under the same conditions for wild type DGK. These results suggest that all mutants are predominantly trimers in the membrane although the trimeric form might be less stable for the mutants A29C and R32C. Comparing these results with the values of v_{max} for the low-activity mutants in Table 1 shows that the low activities for these mutants do not follow just from an inability to form trimers in the membrane.

Fluorescence Properties of NBD-Labeled DGK. Labeling all the Cys-mutants of DGK with IANBD resulted in a labeling ratio for NBD:DGK greater than 0.8:1. Labeling with NBD had only small effects on the activities of the Cys mutants of DGK (Figure 2). Fluorescence emission maxima were determined for NBD-labeled DGK reconstituted into bilayers of di(C18:1)PC (Figure 4). The fluorescence emission maximum for NBD increases with increasing environmental polarity, with a value of 527 nm in a medium of dielectric constant 2, increasing to 547 nm in a medium of

Table 2: Fluorescence Peak Widths for NDB-Labeled Cys Mutants with Low Activities[a]

mutant	emission maximum (nm)	peak width (nm)
E28C	536.0 ± 0.1	65.2 ± 0.2
A29C	534.9	65.9 ± 0.2
A30C	528.4	61.3 ± 0.2
F31C	529.4	61.8 ± 0.1
R32C	527.6	57.2 ± 0.2
Q33C	529.6	61.2 ± 0.2
E34C	528.2	58.9 ± 0.2

[a] Fluorescence emission spectra for DGK in di(C18:1)PC were fitted to the equation for a skewed Gaussian, giving the values for the wavelengths of maximum emission and the peak widths at half-height listed in the table.

dielectric constant 80 (*5*). In bilayers of di(C18:1)PC the labeled mutant with the lowest emission maximum is A41C, suggesting that Ala-41 is likely to be in the middle of the bilayer, with environmental polarity increasing with increasing distance from this residue. The pattern of fluorescence emission is distinctly different for the N-terminal and C-terminal parts of TM1, periodicity being more marked in the C-terminal part. A possible explanation could be that the C-terminal part of TM1 is more tightly packed against the rest of the DGK molecule than is the N-terminal part, and that the observed periodicity in fluorescence emission maxima correspond to faces of TM1 that face the lipid bilayer and face the protein, respectively.

Experiments with the mechanosensitive channel of large conductance, MscL, suggest that an NBD group located just below the glycerol backbone region of a lipid bilayer will show a fluorescence emission maximum at 536.2 nm (*5*). This would define the N-terminal end of TM1 of DGK as being Glu-28 and the C-terminal end as being between Asp-49 and Val-50, with helix TM2 starting at Thr-54 (Figure 4). Fluorescence emission maxima for labeled mutants V50C to I53C are at lower wavelengths than would be expected for an NBD group exposed to water, suggesting that the short loop connecting TM1 and TM2 is located close to the membrane surface, in the lipid headgroup region of the bilayer and partly penetrating into the fatty acyl chain region of the bilayer.

It is important to establish whether or not the spectra recorded for the low-activity mutants correspond to single conformational states for the protein. If the spectra corresponded to the sum of a set of widely different spectra, each arising from one of a set of widely different conformations about the NBD group, it would be very difficult to interpret the fluorescence emission maxima for these mutants. Cross-linking studies show that some of the low-activity mutants give only ca. 60% of the amount of trimer observed for wild type DGK, meaning, however, that ca. 80% of the DGK molecules will be present as trimers, since each trimer contains three DGK molecules (Table 1). Table 2 lists fluorescence emission peak widths at half-height for the low-activity mutants. Ren et al. (*17*) and Ladokhin et al. (*18*) have shown that peak widths for Trp-containing proteins increase with increasing fluorescence emission maximum. The same trend is present in the data in Table 2, the peak width increasing with increasing emission maximum. Importantly, there is no correlation between the extent of trimer formation on cross-linking (Table 1) and the peak width. For example, mutants E28C and A29C show, respectively, 93 and 64% of the amount of trimer formed by wild type DGK, and yet show the same peak widths. This suggests that the mutant A29C exists in a single conformational state as sensed by an NBD group at position 29 since a wider than expected peak would have been observed if the spectrum obtained from labeled A29C was a composite of a set of spectra corresponding to a set of different conformations for the mutant in the membrane.

Table 3: Effect of Molar Ratio of Lipid:DGK on the Fluorescence Emission Maxima for NBD-Labeled Cys Mutants[a]

	fluorescence emission maxima (nm) for labeled mutants			
molar ratio lipid:DGK	E28C	A41C	A46C	D51C
0	536.1 ± 0.1	532.4 ± 0.2	536.3 ± 0.2	539.1 ± 0.1
15:1	538.4 ± 0.1	529.1 ± 0.1	531.1 ± 0.1	534.8 ± 0.1
30:1	537.4 ± 0.1	526.5 ± 0.1	529.7 ± 0.1	534.9 ± 0.1
100:1	536.4 ± 0.1	519.4 ± 0.1	527.9 ± 0.1	533.6 ± 0.3
1000:1	535.5 ± 0.1	518.5 ± 0.1	526.9 ± 0.1	533.4 ± 0.1
3000:1	535.5 ± 0.1	517.8 ± 0.1	527.3 ± 0.1	532.0 ± 0.1

[a] Fluorescence emission spectra for DGK in di(C18:1)PC at the given molar ratios of lipid:DGK were fitted to the equation for a skewed Gaussian, giving the values for the wavelengths of maximum emission listed in the table.

Activity measurements and fluorescence experiments were performed at very different molar ratios of lipid:protein. For the activity measurements, the substrate DHG was contained within the lipid bilayer, and so it was necessary to use a high molar ratio of lipid DGK (6000:1) to ensure that sufficient DHG was present for accurate determinations of steady-state rates. Fluorescence experiments were generally performed at a molar ratio of lipid:DGK of 100:1 to reduce light scatter. The diameter of the transmembrane region of the DGK trimer, containing nine transmembrane α-helices in all, will be similar to that of Ca^{2+}-ATPase, containing ten transmembrane α-helices. The number of lipid molecules required to form a complete annular shell around Ca^{2+}-ATPase is ca. 30 (*2*), so that at a molar ratio of lipid:DGK trimer of 300:1, there will be sufficient lipid to form many shells of lipid molecules around each DGK trimer. Table 3 shows the effect of the molar ratio of lipid:DGK on the fluorescence emission properties of a range of labeled mutants, with the label located close to the glycerol backbone region of the bilayer (E28C, A46C), in the center of the bilayer (A41C) and in an extramembranous loop (D51C). Changes in fluorescence emission maxima are seen for some of the mutants as the molar ratio of lipid:DGK increases from 0 to 30:1, corresponding to the formation of a complete annular shell of lipid molecules around the DGK molecule. However, any changes in emission maxima are small between molar ratios of lipid:DGK of 30:1 and 3000:1 (Table 3). We conclude therefore that the fluorescence properties of labeled DGK recorded at a molar ratio of lipid:DGK of 100:1 correspond to the same state of the DGK molecule reported by the activity measurements recorded at a molar ratio of lipid:DGK of 6000:1.

Effects of Bilayer Thickness. Fluorescence emission maxima for the labeled mutants in bilayers of di(C14:1)PC and di(C22:1)PC are generally very similar to those in di(C18:1)PC (Figure 4). In particular, fluorescence emission maxima for labeled E28C and D49C vary little with lipid chain length, suggesting that these residues remain at the bilayer interface,

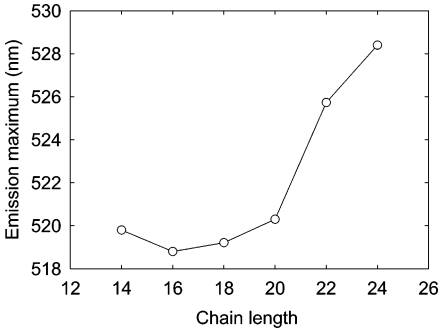

FIGURE 5: Fluorescence properties of NBD-labeled A41C as a function of lipid chain length. Fluorescence emission maxima (nm) are plotted for A41C reconstituted into bilayers of phosphatidylcholine with fatty acyl chains of the given length.

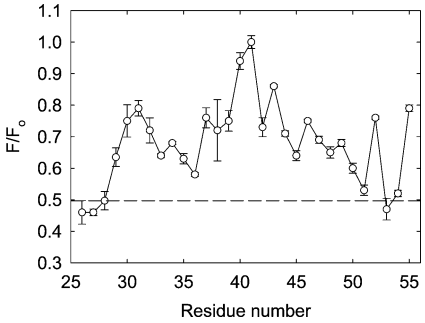

FIGURE 6: Quenching of NBD fluorescence by KI. Values of F/F_0 are plotted as a function of NBD position, where F_0 and F are fluorescence intensities in the absence and presence of 0.45 M KI, respectively. DGK was reconstituted into di(C18:1)PC at a molar ratio of lipid to DGK of 100:1. The dotted line has been drawn through the point for E28C.

despite the change in bilayer thickness resulting from the change in lipid fatty acyl chain length. The largest changes in fluorescence emission maxima are seen for labeled A41C (Figure 4). The variation of fluorescence emission wavelength with fatty acyl chain length for labeled A41C is shown in Figure 5; the fluorescence emission maximum is fairly constant for chain lengths between C14 and C20, but then increases with increasing chain length.

Fluorescence Quenching. Quenching of Trp fluorescence by bromine-containing lipids has been used extensively to study lipid−protein interactions (*19*−*22*), but the fluorescence of the NBD group is not quenched by bromine. NBD fluorescence is, however, quenched by the water-soluble iodide ion (Figure 6). Quenching by 0.45 M KI is very inefficient for labeled L40C and A41C, consistent with a location for these residues in the center of the lipid bilayer. At the N-terminal end of TM1, a large decrease in efficiency of quenching is observed between positions 28 and 30, consistent with a location for these residues close to the bilayer interface. Results are less clear at the C-terminal end of TM1, but the decrease in efficiency of quenching from position 51 to position 49 is again consistent with a location for this region of the protein at the bilayer interface. The inefficiency of quenching for labeled A52C suggests that residue 52 is buried in the hydrophobic core of the bilayer, consistent with the blue-shifted emission spectrum for this residue (Figure 4).

NBD fluorescence is also quenched by nitroxide spin labels. 2,2,6,6-Tetramethylpiperidine-1-oxyl (Tempo) is a water soluble quencher that partitions into lipid bilayers,

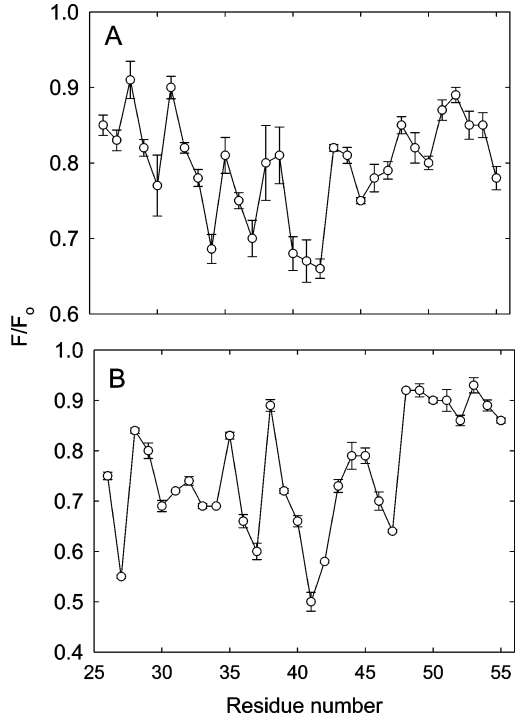

FIGURE 7: Quenching of NBD fluorescence by spin labels. Values of F/F_0 are plotted as a function of NBD position, where F_0 and F are fluorescence intensities in the absence and presence of spin label, respectively: (A) quenching by 2 mM Tempo; (B) quenching by 15 mol % 16-doxyl stearic acid. DGK was reconstituted into di(C18:1)PC at a molar ratio of lipid to DGK of 100:1.

where, as a result of the relatively small volume of the lipid phase, its effective concentration will be high (*23*). It is therefore likely that Tempo will preferentially quench NBD labels in the membrane phase rather than those exposed to the aqueous medium. This is consistent with the observation that quenching of NBD fluorescence by Tempo is greatest for residues between 40 and 42 and is lowest for residues at the N- and C-termini of the proposed helix (Figure 7A). Although the increase in efficiency of quenching between positions 28 and 30 is again consistent with this region of the protein being located close to the bilayer interface, the overall pattern of quenching is complex, with a series of maxima and minima. Quenching of NBD fluorescence by 16-doxyl stearic acid also results in a series of maxima and minima (Figure 7B).

Caputo and London (*24*) showed that taking the ratio of the quenching observed with two different quenchers can emphasize depth-dependent differences between the effects of the two quenchers. Figure 8 shows the ratio of the quenching by the water-soluble iodide quencher and the lipid-soluble nitroxide spin labels. The marked increase in quenching ratio at position 28 is again consistent with a location for Glu-28 close to the glycerol backbone region of the bilayer. Quenching ratios at the C-terminal end of TM1 are more difficult to interpret, but the low quenching ratios between positions 48 and 51 are consistent with the C-terminal end of TM1 being in this region.

Measurements of fluorescence emission maxima detect the largest changes with changing lipid fatty acyl chain length around position 41 (Figure 4). Measurements of the levels of quenching by KI and Tempo also show significant changes in the efficiency of quenching in this region on changing

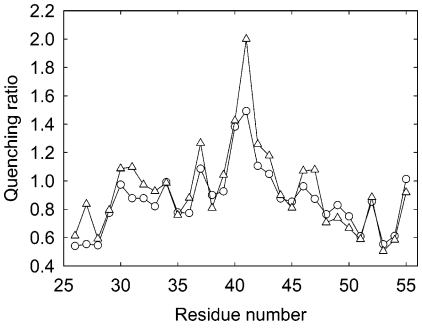

FIGURE 8: Quenching ratios for NBD-labeled DGK. The ratio of the quenching by 0.45 M KI to that by 2 mM Tempo (○) or 15 mol % 16-doxyl stearic acid (△) is plotted as a function of NBD position. Quenching data are from Figures 6 and 7.

from di(C18:1)PC to di(C22:1)PC, an increase in efficiency of quenching by KI in di(C22:1)PC corresponding to a decrease in efficiency of quenching by Tempo (Figure 9).

DISCUSSION

Hydropathy Plots and the Identification of Transmembrane α-Helices. In the absence of a crystal structure, transmembrane α-helices in intrinsic membrane proteins are usually identified from hydropathy plots. Such plots can, however, be misleading if the TM α-helix contains charged residues close to an end of the helix because the charged residues are likely to be assigned to the extramembranous regions of the protein rather than to the region of the protein spanning the hydrophobic core of the lipid bilayer. A well-established example is provided by the Ca^{2+}-ATPase of sarcoplasmic reticulum where charged residues, known to be in TM α-helices from the crystal structure of the protein, are wrongly assigned in hydropathy plots (*4*). It is therefore important to establish experimental methods that can be used to refine the information obtained from hydropathy plots; the method explored here exploits the environmental sensitivity of fluorescence groups such as NBD-labeled Cys residues.

As a test for the approach, we have chosen to study the first TM α-helix of DGK. DGK is predicted to contain three TM α-helices (Figure 1) (*7*). Whereas the C-terminal end of TM1 is well-defined in hydropathy plots as Asp-49, the N-terminal end appears to be defined in hydropathy plots by the charged/polar cluster ^{32}RQE^{35}, resulting in an unusually short TM α-helix of just 14 residues. The highest activity for DGK is observed in a bilayer of lipids with chains C18 in length, for which the hydrophobic thickness is ca. 27 Å (*13*). If it is assumed that highest activity is observed when the hydrophobic thickness of a protein matches that of the surrounding lipid bilayer, the hydrophobic thickness of DGK would then be ca. 27 Å, corresponding to TM α-helices 18 residues in length, or more if the helices were tilted. An alternative possibility is therefore that the N-terminal end of TM1 is actually defined by Glu-28, a conserved residue in the DGK family (*13*), and that the charged/polar residues ^{32}RQE^{35} are buried within the lipid bilayer, the charged groups either snorkeling toward the membrane-water interface or being involved in helix−helix interactions. This would be consistent with NMR studies that suggest that residues 29−47 are helical (*14*). Here we show that fluorescence methods can be used to define the N-terminus of TM1 as Glu-28.

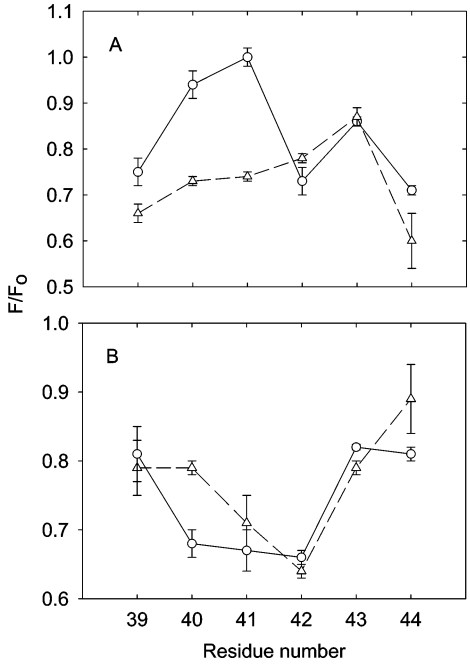

FIGURE 9: Effects of chain length on quenching of NBD fluorescence by KI (A) and Tempo (B). Values of F/F_0 are plotted as a function of NBD position, where F_0 and F are, respectively, fluorescence intensities in the absence and presence of 0.45 M KI (A) and 2 mM Tempo (B). Labeled mutants were reconstituted in di(18:1)PC (○) or di(C22:1)PC (△).

Activities of Cys Mutants. Single Cys mutants of DGK have been produced, spanning the first predicted TM helix and the short loop connecting this to the second predicted TM helix. Mutations at the C-terminal end of TM1 resulted in mutants with high activities, consistent with the observation by Zhou et al. (*25*) that the sequence from Gly-35 to Leu-48 could be replaced by a stretch of Ala residues with only a halving of activity. In contrast, mutations at positions 28−34 resulted in mutants with low activities (Figure 2), as found by Oxenoid et al. (*14*). Previous studies have shown that mutants of DGK are prone to misfolding, as shown by low enzymatic activity, a problem which can, in some cases, be minimized by reconstitution into lipid bilayers (*16*, *26*). In many cases the misfolded DGK fails to form the normal trimeric structure, as shown by cross-linking studies, although some low-activity mutants remain homotrimeric (*26*). A careful study of one low-activity mutant compared values for v_{max} and K_M for ATP with those of wild type enzyme; the finding that v_{max} for the mutant was reduced with no effect on K_M suggested that the sample contained a mixture of correctly folded DGK with normal activity and misfolded DGK that was completely inactive (*26*). This is not the pattern generally seen with the low-activity mutants studied here. Based on cross-linking studies, all the low-activity mutants appear to be predominantly trimeric after reconstitution into lipid bilayers (Table 1). For example, cross-linking mutants A29C and R32C gave about 60% of the amount of trimer observed on cross-linking wild type DGK, meaning that ca. 80% of the DGK molecules for the mutants are present in the trimeric form. For the other low-activity mutants, the proportion of DGK molecules present as trimers was higher than this (Table 1). This suggests that the basic pattern of packing of the TM α-helices is preserved in the low-activity mutants, or they would have failed to pack as

trimers in the membrane. This is also consistent with the measured fluorescence peak widths for the NBD-labeled mutants (Table 2) which suggest that the mutants exist predominantly in a single conformational state, at least as sensed by the NBD group.

Mutants E28C and A29C show a decrease in affinity for ATP and a large decrease in v_{max} compared to wild type DGK, and mutants A30C and E34C show a decrease in affinity for both ATP and DHG, together with a large decrease in v_{max} (Table 1). Mutants F31C, R32C, and Q33C show smaller changes in v_{max} together with some decreases in affinity for ATP and DHG. Of these residues, Glu-28, Ala-30, Phe-31, and Arg-32 are highly conserved. These studies point to the importance of the N-terminal end of TM1 in protein function,because of either a role in catalysis or a structural role (*14*). However, the fact that mutations in this region do not prevent DGK from packing in the trimeric form argues against any major change in the way that the TM helices insert across the membrane.

The First TM Helix of DGK. Fluorescence emission maxima for NBD-labeled Cys mutants of DGK reconstituted into bilayers of di(C18:1)PC (Figure 4) were used to identify residues located close to the glycerol backbone region of the bilayer. There is always a danger, of course, that mutagenesis and labeling will lead to a significant change in the structure of a protein and, for a membrane protein, of how it sits in the lipid bilayer. This is a particular risk when the residue being modified is a charged residue with a role in anchoring a transmembrane α-helix into the bilayer. However, the data shown in Figure 4 suggest that it is not a problem here. For example, replacing the charged or polar Arg, Gln, or Glu residues at positions 32, 33, and 34 respectively with an NBD-labeled Cys results in fluorescence emission maxima very similar to those observed when the nonpolar residue Ala-30 or Phe-31 is replaced by an NBD-labeled Cys residue. Perhaps even more convincing are the results obtained on mutating Glu-28 and Ala-29. Studies with MscL have suggested that an NBD group located close to the glycerol backbone will have a fluorescence emission maximum at 536.2 nm (*5*). The fluorescence emission maximum for DGK with an NBD-labeled Cys at position 29 then locates residue 29 just below the glycerol backbone (Figure 4), TM1 presumably being anchored into the bilayer by Glu-28. When the Glu-28 residue itself is replaced by the NBD-labeled Cys residue, the fluorescence emission maximum increases by just 1 to 536 nm, suggesting that the labeled residue is located in the glycerol backbone region, even though the normal anchoring residue Glu-28 is no longer present. A similar result is seen at the C-terminal end of TM1, where a smooth increase in fluorescence emission maxima is seen on replacing Leu-48, Asp-49, and Val-50 with an NBD-labeled Cys residue (Figure 4), with no discontinuity on replacing Asp-49 of the type that would have been expected if changing this residue had led to a major change in the way that TM1 sits in the membrane. These results therefore argue against any major change in the location of TM1 within the membrane as a result of mutation and labeling. Helix packing in the homotrimeric structure could help to ensure that helices are correctly oriented even when individual residues important in anchoring the helix into the membrane are mutated. A possible example is provided by studies of the role of Trp residues in DGK where

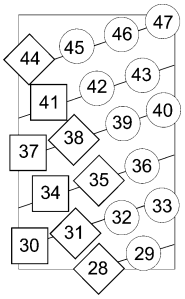

FIGURE 10: Quenching of NBD fluorescence by Tempo and 16-doxyl stearic acid. Residues are plotted on a helical surface with squares representing maxima in quenching by both Tempo and 16-doxyl stearic acid and diamonds representing minima in quenching by both Tempo and 16-doxyl stearic acid. Quenching data are taken from Figure 7.

Trp residues at the membrane−water interface could be mutated with little effect on activity, but with a decrease in the thermal stability of the protein (*12*).

Using a fluorescence emission maximum at 536.2 nm as a marker for an NBD group at the interface (*5*) identifies the region of TM1 spanning the hydrophobic core of the bilayer as running from Glu-28 to Asp-49 or Val-50 (Figure 4). This would be consistent with NMR studies that suggest that residues 29−47 are helical (*14*). If Asp-49 is located at the glycerol backbone region of the bilayer on the periplasmic side of the membrane, then Trp-47 would also be located close to the glycerol backbone region, as suggested from studies of Trp fluorescence (*12*). Glu-34 would then be located within the hydrophobic core of the lipid bilayer, probably snorkeling up to the surface of the bilayer. Mutations in the region between Glu-28 and Glu-34 could then affect packing of helices in this region, possibly explaining why mutations in the region between Glu-28 and Glu-34 have large effects on activity, as described above. The suggestion that the two ends of TM1 are marked by acidic residues, Glu-28 at the N-terminal end and Asp-49 at the C-terminal end, is consistent with the finding that acidic residues are common in crystal structures of membrane proteins in regions likely to correspond to the glycerol backbone region of the surrounding lipid bilayer (*2*).

The NBD results also suggest that TM2 starts at ca. Thr-54 and that the short loop linking these two TM helices is located close to the membrane surface with Ala-52 penetrating into the hydrocarbon core of the bilayer (Figure 4).

Fluorescence quenching results show that accessibility to the iodide ion decreases markedly from position 28 to position 31, consistent with a location for Glu-28 at the interface (Figure 6). Results are less clear at the C-terminal end of TM1, but the increase in efficiency of quenching from labeled D49C to D51C is consistent with the residues in this region being at the interface. The low level of quenching for labeled A52C is consistent with penetration of Ala-52 into the hydrocarbon core of the bilayer.

The pattern of quenching by the lipid-soluble quenchers Tempo and 16-doxyl stearic acid is more complex than that shown by iodide ion, with a series of maxima and minima (Figure 7). These maxima and minima of quenching, when plotted on a helical surface, lie on stripes roughly parallel to the long axis of the helix (Figure 10). This is consistent with a location for TM1 on the outside of the helical bundle

making up the trimeric structure, partly exposed to the lipid bilayer and partly in contact with the rest of the protein. If it is assumed that the face of TM1 that is exposed to the lipid bilayer contains residues that correspond to peaks in quenching by both Tempo and 16-doxyl stearic acid, then the lipid exposed face of TM1 contains residues 30, 34, 37, and 41. Results for NBD-labeled A45C are anomalous, with a small maximum for quenching with Tempo but a minimum in quenching for 16-doxyl stearic acid (Figure 7). Minima in quenching by both Tempo and 16-doxyl stearic acid occur at residues 28, 31, 35, 38, and 44, and would then correspond to residues facing the rest of the DGK protein.

Although the effects are rather small, some of the maxima and minima in quenching correspond to minima and maxima in fluorescence emission wavelengths. Thus minima in quenching at positions 28, 35, 38, and 44 correspond to maxima in fluorescence emission maxima (Figure 4) and maxima in the quenching at positions 37 and 41 corresponding to minima in plots of fluorescence emission maxima (Figure 4). If the maxima and minima in quenching correspond to the most and least lipid exposed residues, respectively, this would imply that the NBD group in a lipid exposed position has a lower fluorescence emission maximum than a residue at an equivalent depth in the bilayer but facing the protein, probably because lipid exposed residues are in more hydrophobic environments than protein exposed residues.

Effects of Bilayer Thickness. The efficiency of hydrophobic matching between DGK and the surrounding lipid bilayer is high since interfacial residues in TM1 maintain their positions against a ca. 14 Å change in bilayer thickness, from di(C14:1)PC to di(C22:1)PC, as shown by the very small changes shown in fluorescence emission maxima for NBD-labeled E28C, D49C, and V50C (Figure 4). This efficient matching could be achieved by distortion of the lipid bilayer around a rigid membrane protein, by distortion of the protein, or by some mixture of the two. The fact that the activity of DGK changes with changing bilayer thickness (*13*) suggests that at least some of the hydrophobic matching is achieved by distortion of the membrane protein, most likely by a change in tilt or bend for the TM α-helices (*27*−*29*).

Changes in fluorescence emission maxima with lipid fatty acyl chain length for labeled residues in the loop region between residues 49 and 54 are very small, and, in particular, the marked shift to lower wavelength observed for labeled A52C is maintained over the lipid chain length range C14 to C22 (Figure 4). This again argues that interfacial residues maintain their positions close to the interface and thus that any distortion of the protein to achieve hydrophobic matching is likely to involve distortion of the TM α-helices.

Surprisingly, the largest changes in fluorescence emission maximum with lipid fatty acyl chain length are observed for labeled A41C where the label will be located toward the center of the lipid bilayer (Figure 4); the fluorescence emission maximum for labeled A41C increases with increasing chain length beyond C20 (Figure 5). The pattern of quenching of residues in the middle of the bilayer by KI and Tempo is also different in di(C18:1)PC and di(C22:1)PC, with increased levels of quenching by KI and decreased levels of quenching by Tempo for labeled L40C and A41C in di(C22:1)PC (Figure 9). If, as suggested above, the high levels of quenching by Tempo observed at positions 40−42 in di(C18:1)PC show that these positions are exposed to the lipid bilayer, the reduced quenching by Tempo at positions 40 and 41 in di(C22:1)PC suggest a conformational change in which these two residues become less lipid exposed, moving them to a location where the accessibility to iodide ion is similar to that for the neighboring residues (Figure 9). The results are also consistent with the trend established above that low quenching by Tempo corresponds to high wavelengths of fluorescence emission maximum.

Table 4: Effect of Lipid Fatty Acyl Chain Length on the Fluorescence Peak Widths for NDB-Labeled A41C[a]

lipid	peak width (nm)
di(C14:1)PC	61.28 ± 0.1
di(C16:1)PC	60.32 ± 0.2
di(C18:1)PC	62.44 ± 0.2
di(C20:1)PC	62.24 ± 0.2
di(C22:1)PC	65.61 ± 0.1
di(C24:1)PC	63.18 ± 0.2

[a] Fluorescence emission spectra for DGK in bilayers of the given lipids at a molar ratio lipid:DGK of 100:1 were fitted to the equation for a skewed Gaussian, giving the values for the peak widths at half-height listed in the table.

An alternative explanation for the changes observed for labeled A41C on increasing lipid chain length could be that, in bilayers whose hydrophobic thickness is too large, a significant proportion of TM1 was unable to span the lipid bilayer and, instead, adopted a non-transmembrane orientation on the bilayer surface. The presence of two major conformational states for TM1 as reported by labeled A41C, one with a blue-shifted spectrum and one with a red-shifted spectrum, would result in a composite fluorescence emission spectrum with a greater than expected spectral width. In fact, the peak width for the fluorescence emission spectrum of labeled A41C did increase from di(C14:1)PC to di(C22:1)-PC (Table 4) but the changes in width were not large and did not vary as smoothly with chain length as did the emission maximum (Figure 5). Further, a change in location for TM1 in di(C22:1)PC would be expected to affect the fluorescence emission properties for NBD at many positions in TM1, and this was not observed (Figure 4). Although a possible location for TM1 not spanning the lipid bilayer in di(C22:1)PC cannot, therefore, be ruled out, it seems less likely than a smaller change in TM1 affecting just positions 40 and 41.

ACKNOWLEDGMENT

We thank Professor James Bowie for the clone for DGK and Professor Charles Saunders for generously sending us the preliminary coordinates for the DGK structure.

REFERENCES

1. White, S. H., Ladokhin, A. S., Jayasinghe, S., and Hristova, K. (2001) How membranes shape protein structure, *J. Biol. Chem. 276*, 32395−32398.
2. Lee, A. G. (2003) Lipid-protein interactions in biological membranes: a structural perspective, *Biochim. Biophys. Acta 1612*, 1−40.
3. Lomize, M. A., Lomize, A. L., Pogozheva, I. D., and Mosberg, H. I. (2006) OPM: Orientations of proteins in membranes database, *Bioinformatics 22*, 623−625.
4. Lee, A. G. (2002) Ca^{2+}-ATPase structure in the E1 and E2 conformations: mechanism, helix-helix and helix-lipid interactions, *Biochim. Biophys. Acta 1565*, 246−266.

5. Powl, A. M., Wright, J. N., East, J. M., and Lee, A. G. (2005) Identification of the hydrophobic thickness of a membrane protein using fluorescence spectroscopy: studies with the mechanosensitive channel MscL, *Biochemistry 44*, 5713−5721.
6. Lakowicz, J. R. (1999) *Principles of Fluorescence Spectroscopy*, Kluwer Academic/Plenum Press, New York
7. Smith, R. L., O'Toole, J. F., Maguire, M. E., and Sanders, C. R. (1994) Membrane topology of *Escherichia coli* diacylglycerol kinase, *J. Bacteriol. 176*, 5459−5465.
8. Lau, F. W., Chen, X., and Bowie, J. U. (1999) Active sites of diacylglycerol kinase from *Escherichia coli* are shared between subunits, *Biochemistry 38*, 5521−5527.
9. Nagy, J. K., Lau, F. W., Bowie, J. U., and Sanders, C. R. (2000) Mapping the oligomeric interface of diacylglycerol kinase by engineered thiol cross-linking: Homologous sites in the transmembrane domain, *Biochemistry 39*, 4154−4164.
10. Badola, P., and Sanders, C. R. (1997) *Escherichia coli* diacylglycerol kinase is an evolutionarily optimized membrane enzyme and catalyzes direct phosphoryl transfer, *J. Biol. Chem. 272*, 24176−24182.
11. Walsh, J. P., and Bell, R. M. (1986) *sn*-1,2-diacylglycerol kinase of *Escherichia coli*. Mixed micellar analysis of the phospholipid cofactor requirement and divalent cation dependence, *J. Biol. Chem. 261*, 6239−6247.
12. Clark, E. H., East, J. M., and Lee, A. G. (2003) The role of tryptophan residues in an integral membrane protein: diacylglycerol kinase, *Biochemistry 42*, 11065−11073.
13. Pilot, J. D., East, J. M., and Lee, A. G. (2001) Effects of bilayer thickness on the activity of diacylglycerol kinase of Escherichia coli, *Biochemistry 40*, 8188−8195.
14. Oxenoid, K., Sonnichsen, F. D., and Sanders, C. R. (2002) Topology and secondary structure of the N-terminal domain of diacylglycerol kinase, *Biochemistry 41*, 12876−12882.
15. Segel, I. H. (1975) *Enzyme Kinetics*, John Wiley & Sons, New York.
16. Gorzelle, B. M., Nagy, J. K., Oxenoid, K., Lonzer, W. L., Cafiso, D. S., and Sanders, C. R. (1999) Reconstitutive refolding of diacylglycerol kinase, an integral membrane protein, *Biochemistry 38*, 16373−16382.
17. Ren, J. H., Lew, S., Wang, Z. W., and London, E. (1997) Transmembrane orientation of hydrophobic α-helices is regulated both by the relationship of helix length to bilayer thickness and by the cholesterol concentration, *Biochemistry 36*, 10213−10220.
18. Ladokhin, A. S., Jayasinghe, S., and White, S. H. (2000) How to measure and analyze tryptophan fluorescence in membrane properly, and why bother?, *Anal. Biochem. 285*, 235−245.
19. East, J. M., and Lee, A. G. (1982) Lipid selectivity of the calcium and magnesium ion dependent adenosinetriphosphatase, studied with fluorescence quenching by a brominated phospholipid, *Biochemistry 21*, 4144−4151.
20. O'Keeffe, A. H., East, J. M., and Lee, A. G. (2000) Selectivity in lipid binding to the bacterial outer membrane protein OmpF, *Biophys. J. 79*, 2066−2074.
21. Williamson, I. M., Alvis, S. J., East, J. M., and Lee, A. G. (2002) Interactions of phospholipids with the potassium channel KcsA, *Biophys. J. 83*, 2026−2038.
22. Powl, A. M., East, J. M., and Lee, A. G. (2003) Lipid-protein interactions studied by introduction of a tryptophan residue: the mechanosensitive channel MscL, *Biochemistry 42*, 14306−14317.
23. Lee, A. G., Birdsall, N. JM., Metcalfe, J. C., Toon, P. A., and Warren, G. B. (1974) Clusters in lipid bilayers and the interpretation of thermal effects in biological membranes, *Biochemistry 13*, 3699−3705.
24. Caputo, G. A., and London, E. (2003) Using a novel dual fluorescence quenching assay for measurment of tryptophan depth within lipid bilayers to determine hydrophobic α-helix locations within membranes, *Biochemistry 42*, 3265−3274.
25. Zhou, Y. F., Wen, J., and Bowie, J. U. (1997) A passive transmembrane helix, *Nat. Struct. Biol. 4*, 986−990.
26. Oxenoid, K., Sonnichsen, F. D., and Sanders, C. R. (2001) Conformationally specific misfolding of an integral membrane protein, *Biochemistry 40*, 5111−5118.
27. Lee, A. G. (2004) How lipids affect the activities of integral membrane proteins, *Biochim. Biophys. Acta 1666*, 62−87.
28. Lee, A. G. (2005) How lipids and proteins interact in a membrane: a molecular approach, *Mol. Biosyst. 1*, 203−212.
29. Powl, A. M., East, J. M., and Lee, A. G. (2007) Different effects of lipid chain length on the two sides of a membrane and the lipid annulus of MscL, *Biophys. J.*, in press.

BI7008213